Structure of glassy and liquid $GeSe_2$

2003 J. Phys.: Condens. Matter 15 S1509

(http://iopscience.iop.org/0953-8984/15/16/301)

INSTITUTE OF PHYSICS PUBLISHING JOURNAL OF PHYSICS: CONDENSED MATTER

J. Phys.: Condens. Matter **15** (2003) S1509–S1528 PII: S0953-8984(03)54779-8

Structure of glassy and liquid $GeSe_2$

Philip S Salmon and Ingrid Petri

Department of Physics, University of Bath, Bath BA2 7AY, UK

Received 15 October 2002
Published 14 April 2003
Online at stacks.iop.org/JPhysCM/15/S1509

Abstract

The partial structure factors of bulk-quenched glassy $GeSe_2$ were measured by using the method of isotopic substitution in neutron diffraction to enable the first detailed comparison at the partial pair distribution function level of a covalently bonded network system in both its glassy and liquid phases. The results show that the basic building block of the glass is the $Ge(Se_{1/2})_4$ tetrahedron in which 34(5)% of the Ge atoms reside in edge-sharing configurations. The intrinsic chemical order of the glass is, however, broken with a maximum of 25(5)% Ge and 20(5)% Se being involved in homopolar bonds at distances of 2.42(2) and 2.32(2) Å, respectively, which is consistent with the existence of these features in the liquid phase of $GeSe_2$. Like for the liquid, concentration fluctuations in the glass are found to extend over distances characteristic of the intermediate-range atomic ordering as manifested by the appearance of a first sharp diffraction peak at 1.00(2) $Å^{-1}$ in the Bhatia–Thornton concentration–concentration partial structure factor. A comparison is made between the measured partial structure factors and recent first principles molecular dynamics simulations for the glassy and liquid phases. It is found that the most significant disagreement between experiment and simulation occurs with respect to the Ge–Ge correlations and that the simulated results for the glass are too liquid-like, reflecting the use of a quench time greatly in excess of that achieved experimentally.

1. Introduction

Network glass forming systems with the AX_2 stoichiometry (A = Si, Ge; X = O, S, Se) are at the heart of many materials of scientific and technological importance (Elliott 1990, Feltz 1993, Boolchand 2000). For a given material, the short ranged atomic ordering is often described by well defined structural units such as $A(X_{1/2})_4$ tetrahedra that link to give an additional level of structural complexity at intermediate ranged distances (Moss and Price 1985, Elliott 1991, Salmon 1994). This complexity can be substantially changed by altering the character of the bonding via a change of the atomic constituents or through an adjustment of the temperature and pressure (e.g. Salmon 1992, Petri *et al* 1999a, Massobrio *et al* 2000b, Crichton *et al* 2001, Durandurdu and Drabold 2002). It is, however, difficult to provide definitive information on the

basic structure and its adaptations owing to the intrinsic difficulties of working with disordered systems. The structure and behaviour of AX_2 systems, on both the short and intermediate ranged atomic length scales, therefore continue to pose a considerable challenge to experiment and theory.

In this paper we tackle the problem of the structure of glassy $GeSe_2$ by applying the method of isotopic substitution in neutron diffraction to measure the full set of partial structure factors, $S_{\alpha\beta}(k)$, where k denotes the magnitude of the scattering vector. The structure of this prototypical glass has long been the subject of controversy, the scope of the proposed models covering two different philosophies. On the one hand, is the basic structure best described in terms of a chemically ordered continuous random network, as originally proposed by Zachariasen (1932), in which homopolar or 'wrong' bonds may occur accidentally (Tronc *et al* 1973, Nemanich *et al* 1983, Sugai 1987, Fischer-Colbrie and Fuoss 1990)? On the other hand, is it best thought of in terms of an aggregate of motifs that maintain a memory of the crystalline phase of the material and in which homopolar bonds exist as an integral part (Bridenbaugh *et al* 1979, Bresser *et al* 1981, Boolchand *et al* 1982, 1983, Boolchand and Phillips 1992)? A preliminary account of this work on glassy $GeSe_2$ is given elsewhere (Petri *et al* 2000).

The essential theory required to understand the diffraction results will first be described. The sample preparation and characterization will then be outlined together with the neutron diffraction experimental method. Next, the neutron diffraction results at both the first-order difference function and partial structure factor level will be presented and discussed with reference to the results obtained for the molten phase of $GeSe_2$ at 784(3) °C (Penfold and Salmon 1990, 1991, 1992) which can be regarded as a 'strong' liquid (Angell 1988, Elliott 1990) unless the temperature is well above its melting point of 736 °C (Stølen *et al* 2002). Finally, the experimental data for both phases will be compared with the results obtained from recent first-principles molecular dynamics simulations made using two different approaches (Drabold *et al* 2003, Massobrio *et al* 2003).

2. Theory

Consider three samples ${}^{N}\mathrm{Ge}^{N}\mathrm{Se}_2$, ${}^{70}\mathrm{Ge}^{N}\mathrm{Se}_2$ and ${}^{73}\mathrm{Ge}^{76}\mathrm{Se}_2$, where N denotes the natural isotopic abundance, that are identical in every respect except for their isotopic compositions. In a neutron diffraction experiment, the coherent scattered intensity for these samples can be represented by the total structure factors ${}^{N}_{N}F(k)$, ${}^{70}_{N}F(k)$ and ${}^{73}_{76}F(k)$, respectively, where in matrix notation

$$\begin{pmatrix} {}^{N}_{N}F(k) \\ {}^{70}_{N}F(k) \\ {}^{73}_{76}F(k) \end{pmatrix} = \begin{pmatrix} 0.0744(4) & 0.2899(8) & 0.2823(6) \\ 0.1111(22) & 0.354(4) & 0.2823(6) \\ 0.0288(5) & 0.276(3) & 0.662(11) \end{pmatrix} \begin{pmatrix} S_{\mathrm{GeGe}}(k) - 1 \\ S_{\mathrm{GeSe}}(k) - 1 \\ S_{\mathrm{SeSe}}(k) - 1 \end{pmatrix}. \quad (1)$$

In this equation the weighting coefficients are quoted in units of barns (1 barn $= 10^{-28}$ m^2) and were calculated using bound coherent scattering lengths of $b({}^{N}\mathrm{Ge}) = 8.185(20)$, $b({}^{70}\mathrm{Ge}) = 10.0(1)$, $b({}^{73}\mathrm{Ge}) = 5.09(4)$, $b({}^{N}\mathrm{Se}) = 7.970(9)$ and $b({}^{76}\mathrm{Se}) = 12.2(1)$ fm (Sears 1992) which correspond to the isotopic enrichments used in the neutron diffraction experiments (see section 3).

By using two total structure factors it is possible to eliminate one of the so-called Faber and Ziman (1965) partial structure factors $S_{\alpha\beta}(k)$. For example, the Se–Se correlations may be eliminated by forming the first-order difference function (in barns)

$$\Delta_{\mathrm{Ge}}(k) = {}^{70}_{N}F(k) - {}^{N}_{N}F(k) = 0.0367(22)[S_{\mathrm{GeGe}}(k) - 1] + 0.064(4)[S_{\mathrm{GeSe}}(k) - 1] \quad (2)$$

while the Ge–Ge correlations may be eliminated by forming the first-order difference function (in barns)

$$\Delta_{Se}(k) = {}^{73}_{76}F(k) - \frac{b^2({}^{73}\mathrm{Ge})}{b^2({}^{N}\mathrm{Ge})}{}^{N}_{N}F(k) = 0.164(3)[S_{GeSe}(k) - 1] + 0.5523(11)[S_{SeSe}(k) - 1]. \tag{3}$$

The full set of set of partial structure factors is obtained from inversion of equation (1) to give

$$\begin{pmatrix} S_{GeGe}(k) - 1 \\ S_{GeSe}(k) - 1 \\ S_{SeSe}(k) - 1 \end{pmatrix} = \begin{pmatrix} -102.1 & 74.3 & 11.8 \\ 42.7 & -26.8 & -6.8 \\ -13.4 & 8.0 & 3.8 \end{pmatrix} \begin{pmatrix} {}^{N}_{N}F(k) \\ {}^{70}_{N}F(k) \\ {}^{73}_{76}F(k) \end{pmatrix}. \tag{4}$$

A measure of the conditioning of this matrix is provided by its normalized determinant $|A_n| = 0.011$ (Edwards *et al* 1975). This compares, for example, with $|A_n| = 0.018$ for the isotopic substitution experiment of Biggin and Enderby (1981) on molten $ZnCl_2$ in which the full set of $S_{\alpha\beta}(k)$ were successfully measured using the first generation neutron diffraction apparatus at Harwell. The partial structure factors are related to the partial pair distribution functions, $g_{\alpha\beta}(r)$, through

$$g_{\alpha\beta}(r) = 1 + \frac{1}{2\pi^2 n_0 r}\int_0^\infty \mathrm{d}k\,[S_{\alpha\beta}(k) - 1]k\sin(kr) \tag{5}$$

where n_0 (=0.0334(1) Å^{-3}Azoulay *et al* (1975)) is the atomic number density of the glass. The difference functions in real space, corresponding to equations (2) and (3), are therefore given (in barns) by

$$\Delta G_{Ge}(r) = 0.0367(22)[g_{GeGe}(r) - 1] + 0.064(4)[g_{GeSe}(r) - 1] \tag{6}$$

and

$$\Delta G_{Se}(r) = 0.164(3)[g_{GeSe}(r) - 1] + 0.5523(11)[g_{SeSe}(r) - 1] \tag{7}$$

respectively. The mean number of particles of type β contained in a volume defined by two concentric spheres of radii r_i and r_j, centred on a particle of type α, is given by

$$\bar{n}^{\beta}_{\alpha} = 4\pi n_0 c_\beta \int_{r_i}^{r_j} \mathrm{d}r\, g_{\alpha\beta}(r) r^2 \tag{8}$$

where c_β is the atomic fraction of chemical species β.

In practice, the reciprocal space data sets will be limited by the finite measurement window function $M(k)$ of the diffractometer where $M(k \leqslant k_{max}) = 1$, $M(k > k_{max}) = 0$ and $k_{max} = 15.9$ Å^{-1} in the present experiment. In r-space the $M(k)$ function is represented by

$$M(r) = \frac{1}{\pi}\int_0^{k_{max}} \mathrm{d}k\cos(kr) = \frac{k_{max}}{\pi}\mathrm{sinc}(k_{max}r) \tag{9}$$

with $\mathrm{sinc}(x) \equiv \sin(x)/x$. In the case of the partial pair distribution functions it is then convenient (from the viewpoint of fitting the data—see section 4) to consider the function

$$d'_{\alpha\beta}(r) = \frac{2}{\pi}\int_0^\infty \mathrm{d}k\,[S_{\alpha\beta}(k) - 1]kM(k)\sin(kr) = d_{\alpha\beta}(r) \otimes M(r) \tag{10}$$

where $d_{\alpha\beta}(r) = 4\pi n_0 r[g_{\alpha\beta}(r) - 1]$ and $\otimes$ denotes the one-dimensional convolution operator. Throughout this paper, primes will be used to denote r-space functions for which the effect of the finite measurement window is implicit, e.g. $rg'_{\alpha\beta}(r) = rg_{\alpha\beta}(r) \otimes M(r)$ and $r\Delta G'_{Ge}(r) = r\Delta G_{Ge}(r) \otimes M(r)$.

It is also informative to decompose a total structure factor in terms of the Bhatia and Thornton (1970) number–number, concentration–concentration and number–concentration partial structure factors denoted by $S_{NN}^{BT}(k)$, $S_{CC}^{BT}(k)$ and $S_{NC}^{BT}(k)$, respectively, where

$$F(k) = \langle b\rangle^2[S_{NN}^{BT}(k) - 1] + c_{\mathrm{Ge}}c_{\mathrm{Se}}(b_{\mathrm{Ge}} - b_{\mathrm{Se}})^2[\{S_{CC}^{BT}(k)/c_{\mathrm{Ge}}c_{\mathrm{Se}}\} - 1] + 2\langle b\rangle(b_{\mathrm{Ge}} - b_{\mathrm{Se}})S_{NC}^{BT}(k) \tag{11}$$

and $\langle b\rangle = c_{\mathrm{Ge}}b_{\mathrm{Ge}} + c_{\mathrm{Se}}b_{\mathrm{Se}}$ is the average scattering length. The Fourier transform of $S_{NN}^{BT}(k)$, $g_{NN}(r)$, describes the sites of the scattering nuclei and does not distinguish between them. It is measured directly if the bound coherent scattering lengths of the different nuclei are equal, which is almost the case for the $^{N}\mathrm{Ge}^{N}\mathrm{Se}_2$ measurement. The $S_{NN}^{BT}(k)$ function is therefore known to good precision and advantage of this fact has been used to study the evolution with composition and temperature of the topology of liquid and glassy Ge–Se systems using neutron diffraction (Salmon and Liu 1994, Petri *et al* 1999a, Petri and Salmon 2002). The Fourier transform of $S_{CC}^{BT}(k)$, $g_{CC}(r)$, gives information on the decoration by the Ge and Se chemical species of the sites described by $g_{NN}(r)$. When chemical ordering occurs on a given length scale, corresponding features will appear in $S_{CC}^{BT}(k)$. The Fourier transform of $S_{NC}^{BT}(k)$ relates to the correlation between sites and their occupancy by a given chemical species. A fuller description of AX_2 systems within the Bhatia–Thornton formalism is given elsewhere (Salmon 1992).

3. Experimental procedure

The isotopes were freshly separated and immediately sealed under vacuum in glass ampoules for transportation to our laboratory to minimize the chemical impurity content at $\leqslant 0.05\%$. The samples, whose stoichiometry was determined by mass to be 0.3333(2) Ge: 0.6667(2) Se, were prepared identically by loading into silica ampoules ^{N}Ge (99.9999%, Aldrich), ^{70}Ge (99.8% ^{70}Ge, 0.2% ^{72}Ge) or ^{73}Ge (98% ^{73}Ge, 0.3% ^{70}Ge, 0.8% ^{72}Ge, 0.8% ^{74}Ge, 0.1% ^{76}Ge) together with ^{N}Se (99.999%, Johnson Matthey) or ^{76}Se (99.75% ^{76}Se, 0.2% ^{74}Se, 0.05% ^{77}Se) in a high purity argon filled glove box ($\approx$1 ppm oxygen, $<$10 ppm water). The ampoules, of a size (1 mm wall thickness, 4.8 mm internal diameter) chosen to promote the formation of homogeneous glasses, had been cleaned by using chromic acid prior to etching with a 40% solution of hydrofluoric acid. The sample-filled ampoules were then evacuated to a pressure of $\approx 10^{-5}$ Torr, purged three times with helium gas, and after $\approx$48 h they were sealed. Next, the ampoules were loaded into a rocking furnace and were heated at 1 °C min^{-1} to 1000 °C, pausing for 1 h at both the melting and boiling points of Se and the melting point of Ge. After 48 h the ampoules were slowly cooled to 850 °C where they were equilibrated for $\approx$4 h and quenched in an ice/salt water mixture at -5 °C. The glasses separated cleanly from the silica ampoules and were fully amorphous (see section 4) which is consistent with a negligible oxygen contamination. The glass transition temperature of the as-quenched samples was measured to be 394(6) °C (onset) using a TA Instruments Thermal Analyst 2000 machine operating at a scan rate of 10 °C min^{-1}. A single vanadium container of 4.8 mm internal diameter and 0.1 mm wall thickness was chosen to hold the samples for the diffraction experiments which were made using the D4B instrument at the Institut Laue-Langevin, Grenoble, operating with an incident wavelength of 0.7046 Å.

The complete diffraction experiment comprised the measurement of the scattering intensities at 26(1) °C for the samples in their container and the empty container. Each diffraction pattern was built up by making repeated scans of the detectors over the available range of scattering angles. No deviations were observed between scans, apart from the expected statistical variations (Jal *et al* 1990). The intensity for a cadmium neutron-absorbing rod of

similar diameter to the sample was also measured to account for the effect of the sample self-shielding on the background count rate at small scattering angles (Bertagnolli *et al* 1976). The diffraction pattern for a vanadium rod of diameter 6 mm was used for the data normalization and the data analysis procedure followed that described elsewhere (Salmon 1988, Salmon *et al* 1998).

Although the glassy samples used for the diffraction experiments were always handled under high purity argon gas, they were kept in the form of coarsely ground lumps in order to minimize their surface area and thereby the risk of any contamination. An iterative procedure was therefore adopted for the data analysis in which a first estimate of the effective number density of a sample was obtained by measuring its packing fraction in the vanadium container. Self-consistency checks on the resultant $F(k)$ were then applied to ascertain whether it has the correct high-k limit, obeys the usual sum-rule relation and produces a well-behaved real-space function (Salmon and Benmore 1992, Salmon *et al* 1998). The latter should oscillate about the correct low-r limit and the back Fourier transform obtained after setting the unphysical low-r oscillations to this limit should be in good overall agreement with the original k-space function. If necessary, the effective sample number density was then changed and the entire data analysis procedure repeated until the resultant $F(k)$ satisfied these checks. Benmore (1993) confirmed the efficacy of this procedure by making two diffraction experiments using the same instrument on the same glass but with a different sample packing fraction during two different experimental periods. The resultant total structure factors were, within the precision of the measurements ($\pm 0.5\%$), in agreement over the entire k-space range and were used in conjunction with other data sets to construct first-order difference functions. No systematic error resulting from the use of a coarsely powdered sample could be identified at either the total structure factor or first-order difference function level. Moreover, second-order difference functions have been successfully measured for coarsely ground isotopically enriched glassy samples, many containing absorbing isotopes that result in large attenuation corrections (Benmore and Salmon 1994, Liu and Salmon 1997, Salmon *et al* 1998, Salmon and Xin 2002).

4. Results

The measured total structure factors in figure 1 feature a so-called first sharp diffraction peak (FSDP) at 1.00(2) $Å^{-1}$ for $^{N}Ge^{N}Se_2$ and $^{70}Ge^{N}Se_2$ and at 0.99(2) $Å^{-1}$ for $^{73}Ge^{76}Se_2$ which increases in intensity with increasing Ge scattering length. The FSDP remains as a prominent feature at 1.00(2) $Å^{-1}$ in the first-order difference function $\Delta_{Ge}(k)$, where the Se–Se correlations are absent, but is only a small feature at 0.98(2) $Å^{-1}$ in $\Delta_{Se}(k)$, where the Ge–Ge correlations are absent (figure 2). This demonstrates that the intermediate ranged atomic ordering in $GeSe_2$ is associated primarily with the Ge–Ge correlations, an observation that is consistent with differential anomalous x-ray scattering (DAS) experiments on the glassy phase (Fuoss *et al* 1981, Fischer-Colbrie and Fuoss 1990) and with neutron diffraction experiments on the liquid phase (Penfold and Salmon 1990, 1991).

The real-space difference functions $\Delta G'_{Ge}(r)$ and $\Delta G'_{Se}(r)$ are shown in figure 3. By comparison with the so-called high-temperature (HT) crystalline polymorph of $GeSe_2$ (Dittmar and Schäfer 1976), which is the phase that coexists with the liquid at ambient pressure (Crichton *et al* 2001), the dominant local structural motif in the glassy phase will be the $Ge(Se_{1/2})_4$ tetrahedron. Integration of the first peak in $\Delta G'_{Ge}(r)$ at 2.36(2) Å over the range $2.09 \leqslant r$ (Å) $\leqslant 2.61$ and assuming exclusive heteropolar bonding gives $\bar{n}^{Se}_{Ge} = 4.1(1)$ while integrating the first peak in $\Delta G'_{Se}(r)$ at 2.35(2) Å over the same range gives $\bar{n}^{Se}_{Ge} = 4.7(1)$. As will be shown by the full partial pair distribution function analysis of the data, this enhancement of the coordination number above four can be attributed to the presence of homopolar bonds.

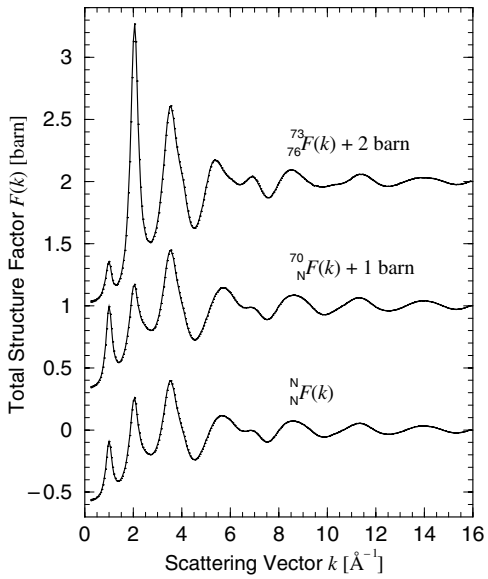

Figure 1. The measured total structure factors, $F(k)$, for glassy $GeSe_2$ at 26(1) °C defined by equation (1). The statistical errors on the data points are smaller than the line width.

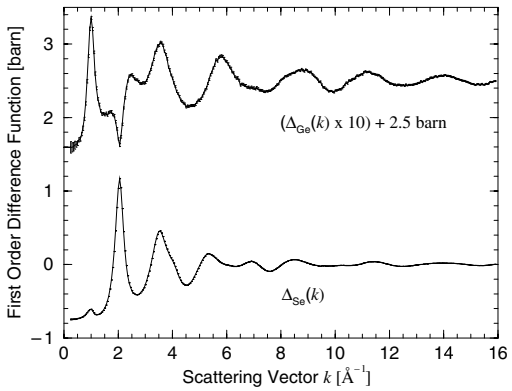

Figure 2. The measured first-order difference functions $\Delta_{Ge}(k)$ and $\Delta_{Se}(k)$ for glassy $GeSe_2$ defined by equations (2) and (3), respectively. The vertical bars give the statistical errors on the data points and are comparable to the curve thickness at most k values.

The second peak in $\Delta G'_{Ge}(r)$ occurs at 3.62(2) Å while the second peak in $\Delta G'_{Se}(r)$ occurs at 3.89(2) Å. This shift, which is consistent with the DAS results of Fischer-Colbrie and Fuoss (1990), points to a first main peak in $g_{GeGe}(r)$ that occurs at a lower value of r than the first main peak in $g_{SeSe}(r)$.

The partial structure factors shown in figure 4, obtained by direct inversion of the total structure factors using equation (4), are of high statistical quality and fully satisfy the sum rule and inequality relations given by Edwards *et al* (1975). As required, they give rise to $g'_{\alpha\beta}(r)$ that oscillate about the correct low-r $g_{\alpha\beta}(r) = 0$ limit and the $S_{\alpha\beta}(k)$ are also in good agreement with the back Fourier transforms of the corresponding $g'_{\alpha\beta}(r)$ after the low-r oscillations are set to this limit (Salmon and Benmore 1992). Furthermore, the total structure factors can be

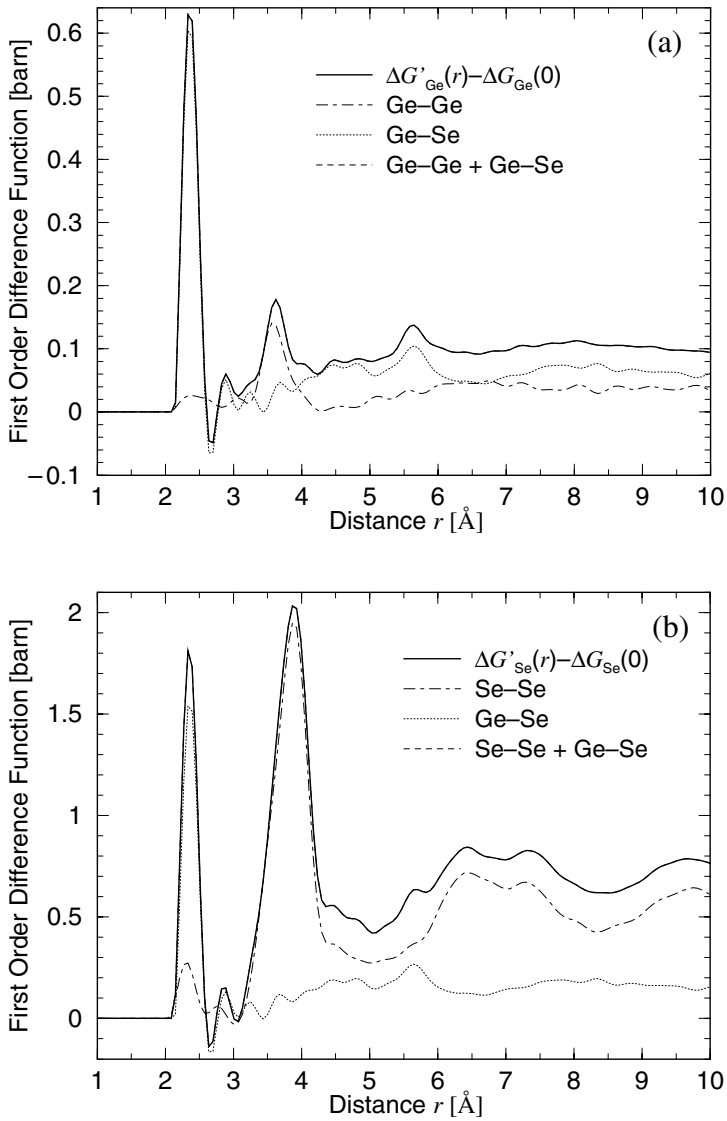

Figure 3. The first-order difference functions $\Delta G'_{Ge}(r)$ and $\Delta G'_{Se}(r)$ for glassy $GeSe_2$ obtained by direct Fourier transformation of the reciprocal space functions given by the curves in figure 2. In (a) $\Delta G'_{Ge}(r)$ is compared with the neutron weighted sum of $g'_{GeGe}(r)$ and $g'_{GeSe}(r)$ (see equation (6)) while in (b) $\Delta G'_{Se}(r)$ is compared with the neutron weighted sum of $g'_{SeSe}(r)$ and $g'_{GeSe}(r)$ (see equation (7)) where the $g'_{\alpha\beta}(r)$ were obtained by direct Fourier transformation of the partial structure factors given by the points with error bars in figure 4. On the scale of the diagram there is no significant discrepancy between the measured difference functions and the weighted sums. Note that the homopolar Ge–Ge and Se–Se bonding features are required to reproduce the first peaks in $\Delta G'_{Ge}(r)$ and $\Delta G'_{Se}(r)$, respectively.

accurately reconstructed from the $S_{\alpha\beta}(k)$ by using equation (1) and the first-order difference functions can also be properly accounted for (see figure 3). The latter point is important since several types of systematic error are reduced or essentially eliminated when forming the Ge first-order difference function (Penfold and Salmon 1990, Salmon and Benmore 1992, Petri *et al* 1999b) and the $S_{Ge\beta}(k)$ functions are the least well conditioned of the set of three.

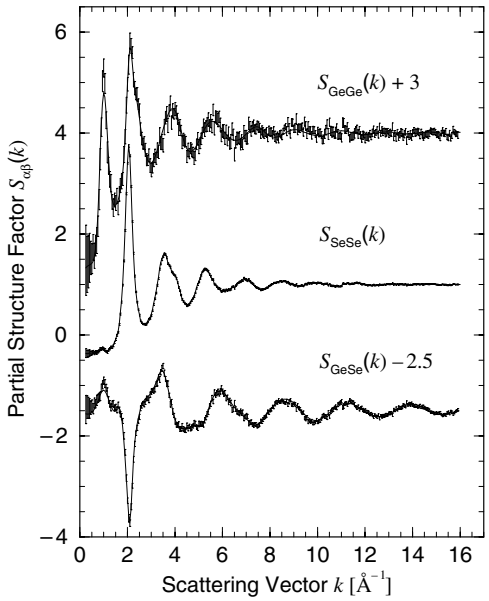

Figure 4. The measured partial structure factors, $S_{\alpha\beta}(k)$, for glassy $GeSe_2$. The bars represent the statistical errors on the data points and the full curves are the back Fourier transforms of the $g_{\alpha\beta}(r)$ given by the full curves in figure 6.

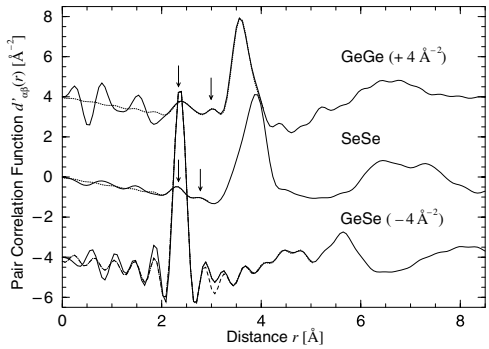

Figure 5. The $d'_{\alpha\beta}(r)$ functions obtained from the $S_{\alpha\beta}(k)$ in figure 4 by spline fitting and Fourier transforming (full curves) and the Gaussian fits (dotted curves). The fitted functions are identical to the measured $d'_{\alpha\beta}(r)$ at larger r values and the vertical arrows point to the fitted low-r features for the like-atom correlations. The broken curve shows the effect of omitting the defect peak at 3.02 Å in the Ge–Se correlations and gives the broken curve in figure 6(b).

Each partial structure factor shows an FSDP, at 1.00(1) Å^{-1} in $S_{GeGe}(k)$ and $S_{GeSe}(k)$ or at 0.95(2) Å^{-1} in $S_{SeSe}(k)$, which is largest for $S_{GeGe}(k)$. They confirm that the FSDP in the measured $F(k)$, which is a ubiquitous feature of covalently bonded amorphous solids (Elliott 1991), arises predominantly from the Ge–Ge correlations, i.e. from the real-space intermediate-range ordering of the Ge-centred structural motifs, although there is also a notable contribution from Ge–Se correlations.

The effects of statistical noise and $M(r)$ complicate an interpretation of the features in the measured $g'_{\alpha\beta}(r)$ functions. The effect of statistical noise was reduced by using spline-fitted partial structure factors for the Fourier transforms. To enable those features that are artefacts of $M(r)$ to be distinguished, the resultant $d'_{\alpha\beta}(r)$, which are shown in figure 5, were fitted by least

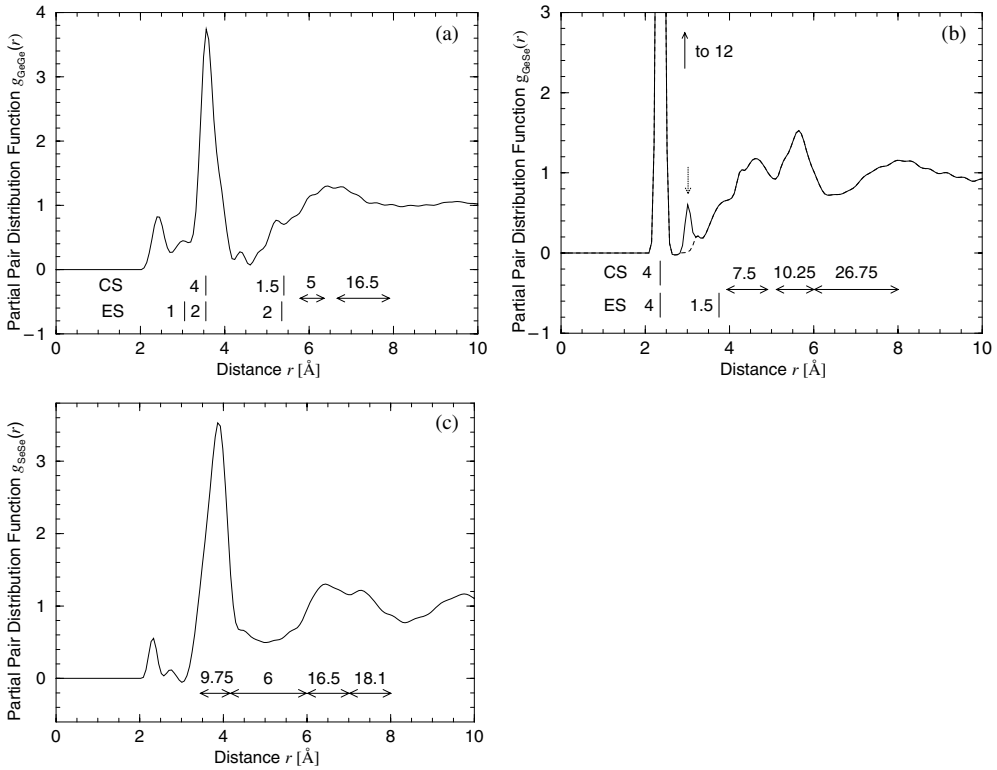

Figure 6. The final $g_{\alpha\beta}(r)$ obtained by fitting the $d'_{\alpha\beta}(r)$ functions of figure 5. Vertical bars show the positions, or horizontal arrows show the spread in positions, of neighbours in the HT crystalline phase of $GeSe_2$ (Dittmar and Schäfer 1976); the adjacent numerals are the corresponding coordination numbers. Since the Ge atom coordination environment has a marked dependence on whether it occupies an edge or corner sharing (ES or CS) site, these two cases have been distinguished at smaller r values for $g_{GeGe}(r)$ and $g_{GeSe}(r)$. The vertical broken arrow in (b) points to the defect peak at 3.02 Å in $g_{GeSe}(r)$ and the broken curve shows the effect of its removal.

Table 1. The R factors obtained from the Gaussian fits to $d'_{\alpha\beta}(r)$ (see figure 5) and the reduced χ^2 values obtained by comparing the experimental data for each $S_{\alpha\beta}(k)$ with the back Fourier transform of the corresponding $g_{\alpha\beta}(r)$ (see figure 4). In the fitting procedure, defect features (Ge–Ge and Se–Se homopolar bonds and the peak at 3.02 Å for Ge–Se) were either (a) included or (b) excluded.

Fitted pair correlations	Type of fit	R factor	Range of fit (Å)	χ^2
Ge–Ge	(a)	0.165	2.09–4.17	0.84
	(b)	37.16		1.04
Ge–Se	(a)	0.498	2.15–5.15	1.14
	(b)	2.928		1.65
Se–Se	(a)	0.002	2.02–2.95	0.40
	(b)	2.784		3.92

squares to a sum of Gaussians representing the partial pair correlation functions convoluted with $M(r)$, namely

$$d'_{\alpha\beta}(r) = \left[\sum_i \frac{\bar{n}^{\beta}_{\alpha}(\mathrm{i})}{\sqrt{2\pi}c_\beta r_{\alpha\beta}(\mathrm{i})\sigma_{\alpha\beta}(\mathrm{i})} \exp\left(\frac{-(r - r_{\alpha\beta}(\mathrm{i}))^2}{2\sigma^2_{\alpha\beta}(\mathrm{i})}\right)\right] \otimes M(r) - 4\pi n_0 r \qquad (12)$$

Table 2. The first few peak positions and corresponding coordination numbers for the glassy (present work) and liquid (Penfold and Salmon 1991) phases of $GeSe_2$.

Phase	$g_{\alpha\beta}(r)$	Peak position (Å)	$\bar{n}_\alpha^\beta$	Integration range (Å)	Peak position (Å)	$\bar{n}_\alpha^\beta$	Integration range (Å)	Peak position (Å)	$\bar{n}_\alpha^\beta$	Integration range (Å)
Glass	$g_{GeGe}(r)$	2.42(2)	0.25(5)	0–2.73	3.02(2)	0.34(5)	2.73–3.19	3.57(2)	3.2(3)	3.19–4.23
	$g_{GeSe}(r)$	2.36(2)	3.7(1)	2.09–2.61						
	$g_{SeSe}(r)$	2.32(2)	0.20(5)	0–2.55	2.74(2)	0.06(3)	2.55–3.09	3.89(2)	9.3(2)	3.09–4.39
Liquid	$g_{GeGe}(r)$	2.33(3)	0.25(10)	0–2.6	—	—	—	3.59(2)	2.9(3)	2.6–4.2
	$g_{GeSe}(r)$	2.42(2)	3.5(2)	0–3.1	4.15(10)	4.0(3)	3.1–4.5			
	$g_{SeSe}(r)$	2.30(2)	0.23(5)	0–2.7	—	—	—	3.75(2)	9.6(3)	2.7–4.8

where $r_{\alpha\beta}(\mathrm{i})$, $\sigma_{\alpha\beta}(\mathrm{i})$ and $\bar{n}_\alpha^\beta(\mathrm{i})$ are the position, standard deviation and coordination number of the ith Gaussian. The quality of fit was measured by the R factor:

$$R = \sum_j \left(\frac{[d'_{\alpha\beta}(r_j)]_{exp} - [d'_{\alpha\beta}(r_j)]_{fit}}{[d'_{\alpha\beta}(r_j)]_{exp}} \right)^2 \tag{13}$$

where the sum is taken over the data points in the fitted region. The final $d_{\alpha\beta}(r)$ were then obtained by smoothly merging the Gaussian representation of $d'_{\alpha\beta}(r)$ in the region where the effect of $M(r)$ is measurable with the $d'_{\alpha\beta}(r)$ obtained by direct Fourier transformation of the spline-fitted $S_{\alpha\beta}(k)$ and by setting the unphysical low-r oscillations to $-4\pi n_0 r$. The resultant $g_{\alpha\beta}(r)$ functions are shown in figure 6 and the R factors are summarized in table 1. As required, the back Fourier transforms of the final $g_{\alpha\beta}(r)$ give an excellent account of the measured $S_{\alpha\beta}(k)$ as shown in figure 4 (the corresponding reduced χ^2 factors are given in table 1).

5. Discussion

5.1. Structure of glassy $GeSe_2$

The main peaks in $g_{GeSe}(r)$, $g_{GeGe}(r)$ and $g_{SeSe}(r)$ at 2.36(2), 3.57(2) and 3.89(2) Å in figure 6 give Ge–Se, Ge–Ge and Se–Se coordination numbers of 3.7(1), 3.2(3) and 9.3(2), respectively, which are comparable to those previously measured for the liquid phase (see table 2). Since the ratio of Ge–Se:Se–Se distances is 0.607(6), close to the value of $\sqrt{3/8} = 0.612$ expected for perfect tetrahedral coordination, the results imply that there are a large number of tetrahedral $Ge(Se_{1/2})_4$ structural motifs. These are the basic building blocks of the HT crystalline phase of $GeSe_2$ (Dittmar and Schäfer 1976) and appear to be more regular in the glass than in the liquid where the distance ratio is 0.645(6). In this crystalline phase, the presence of equal numbers of edge sharing (ES) and corner sharing (CS) $Ge(Se_{1/2})_4$ tetrahedra gives two nearest-neighbour Ge–Ge distances at 3.05 and 3.55 Å, the shortest between the centres of ES motifs (see figure 6(a)). The low-r Ge–Ge peak at 3.02(2) Å for the glass is assigned to this distance and the coordination number of 0.34(5) is consistent with a ratio for the number of Ge in ES tetrahedra, N_{Ge} (ES), to the total number of Ge, N_{Ge}, of 34(5)% in accordance with several other estimates (table 3).

A more complete comparison of the glass and HT-$GeSe_2$ structures is given in figure 6 where the nearest-neighbour Ge centred correlations in the latter, which arise from ES and CS $Ge(Se_{1/2})_4$ motifs, are distinguished. In the case of the Ge–Ge correlations the coordination number $\bar{n}_{Ge}^{Ge} = 3.2(3)$ obtained by integrating the main peak in $g_{GeGe}(r)$ at 3.57(2) Å and excluding the contribution from ES sites at 3.02(2) Å compares with an average Ge–Ge

Table 3. Description of the Ge centred correlations in bulk-quenched glassy $GeSe_2$ in terms of the fraction of Ge involved in ES tetrahedral or dimer-like structural motifs, the ratio of ES to CS $Ge(Se_{1/2})_4$ tetrahedral motifs and the fraction of Ge–Ge homopolar bonds.

$\frac{N_{Ge}(ES)}{N_{Ge}}$ (%)	$\frac{N_{Ge}(dimer)}{N_{Ge}}$ (%)	$\frac{N_{Ge}(ES)}{N_{Ge}(CS)}$ (%)	$\frac{N_{Ge-Ge}}{N_{bond}}$ (%)	Method	Reference
25	—	33	—	X-ray diffraction	Feltz *et al* (1985)
—	16(1)	—	2.0(1)	Mössbauer	Boolchand *et al* (1982)
32	—	47	—	Molecular dynamics	Vashishta *et al* (1989a)
40	—	67	—	Neutron diffraction	Susman *et al* (1990)
—	15(5)	—	1.9(6)	Mössbauer	Peters and McNeil (1992)
40	25	114	3.5	Molecular dynamics	Cobb *et al* (1996), Zhang and Drabold (2000)
—	—	—	6	X-ray emission spectroscopy	Mamedov *et al* (1996)
33	9	57	—	Molecular dynamics	Jackson *et al* (1999)
34(5)	25(5)	83(16)	4(1)	Neutron diffraction	Petri *et al* (2000) and present work
28(2)	15(2)	50(3)	1.9(3)	Raman[a]	Boolchand and Bresser (2000)
—	14(1)	—	1.8(2)	Mössbauer	Boolchand and Bresser (2000)
28(3)	—	39(4)	—	Inelastic neutron scattering	Sinclair *et al* (2002)

[a] Data analysed using the Raman cross-sections calculated by Jackson *et al* (1999).

coordination number of 3 in HT-$GeSe_2$. For the Ge–Se correlations, the position of the first peak in $g_{GeSe}(r)$ agrees with the value found in HT-$GeSe_2$ although the corresponding Ge–Se coordination number of 3.7(1) is less than 4. The shoulder at $\approx$3.7 Å found in $g_{GeSe}(r)$ coincides with the correlations associated with ES sites in the crystal which supports the existence of these configurations in the glass. In the case of the Se–Se correlations, the coordination number $\bar{n}^{Se}_{Se}$ = 9.3(2) obtained for the glass by integrating over the range $3.09 \leqslant r$ (Å) $\leqslant 4.39$ compares with an Se–Se coordination number of 9.75 found between 3.45 and 4.16 Å in the crystal. Overall, the comparison of figure 6 shows that the short-range order in the glass has many features similar to HT-$GeSe_2$ although there are significant differences in detail.

Importantly, there is clear evidence for a substantial number of defects, i.e. structural motifs that are *not* present in HT-$GeSe_2$. For example, the like-atom $g_{\alpha\beta}(r)$ show Ge–Ge and Se–Se correlations at typical homopolar single bond distances of 2.42(2) and 2.32(2) Å, respectively (Zhou *et al* 1991, Petri *et al* 1999c, Choi *et al* 2002). These small-r features are evident in the $g'_{\alpha\beta}(r)$, i.e. they are not artefacts of the fitting procedure, and as shown in figure 3 they are required if the first peaks in $\Delta G'_{Ge}(r)$ and $\Delta G'_{Se}(r)$ are to be reproduced by using the measured $g'_{\alpha\beta}(r)$. Furthermore, their removal has a deleterious effect on the agreement between the back Fourier transform of the like-atom $g_{\alpha\beta}(r)$ and the corresponding $S_{\alpha\beta}(k)$, as shown by the reduced χ^2 values in table 1. The coordination numbers for the Ge–Ge and Se–Se homopolar bonds are 0.25(5) and 0.20(5), comparable to the values found in the liquid phase (table 2). The total Ge and Se coordination numbers, $\bar{n}_{Ge} = \bar{n}^{Se}_{Ge} + \bar{n}^{Ge}_{Ge}$ and $\bar{n}_{Se} = \bar{n}^{Ge}_{Se} + \bar{n}^{Se}_{Se}$, are therefore 4.0(1) and 2.05(7), respectively. Hence Ge and Se are, within experimental error, four-fold and two-fold coordinated, i.e. they have a full outer shell of eight electrons.

If only dimers are formed, then the maximum fraction of Ge involved in homopolar bonds, $N_{Ge}(dimer)/N_{Ge}$, is 25(5)% and the maximum fraction of Se involved in homopolar bonds, $N_{Se}(dimer)/N_{Se}$, is 20(5)%. The number of Ge–Ge (N_{Ge-Ge}) or Se–Se (N_{Se-Se}) homopolar bonds is roughly the same at 0.05(2) N', where N' is the total number of atoms, and the total number of bonds in $GeSe_2$, N_{bond}, is $4N'/3$ if the bonding requirements of Ge and Se are fully satisfied. Hence the ratio of the number of Ge–Ge (or Se–Se) bonds to the total

number of bonds in the glass, $N_{\mathrm{Ge-Ge}}/N_{tot}$, is 4(1)%, which is in agreement with an estimate of 4.2% based on the law of mass action (Feltz 1985). Although the presence of defects in bulk-quenched glassy $GeSe_2$ has been inferred from other experimental methods (table 3), like Raman (Nemanich *et al* 1978, Bridenbaugh *et al* 1979, Jackson *et al* 1999, Murase 2000, Boolchand and Bresser 2000) and Mössbauer spectroscopy (Bresser *et al* 1981, Boolchand *et al* 1982, Boolchand *et al* 1983, Peters and McNeil 1992—also see Jackson *et al* (2002) for a recent theoretical interpretation of Mössbauer data using Sn as a Ge probe), their existence has proved controversial (Tronc *et al* 1973, Nemanich *et al* 1983, Sugai 1987) and they have not previously been identified by using diffraction (Fischer-Colbrie and Fuoss 1990, Susman *et al* 1990) or extended x-ray absorption fine structure (Zhou *et al* 1991) methods[1]. This is a consequence, in part, of the similar neutron scattering lengths for Ge and Se of natural isotopic abundance and their close atomic numbers and sizes.

Application of the method of isotopic substitution in neutron diffraction has, however, enabled these important structural features to be resolved and will thus allow for a better test of various scenarios for the origin of the intrinsic broken chemical order. These include the nanoscale phase separation model of Boolchand and co-workers (Boolchand and Bresser 2000), which originates from the disputed 'outrigger raft' model (Bridenbaugh *et al* 1979, Boolchand *et al* 1982, Bresser *et al* 1986), in which the predominant Ge-centred structural motifs are regular $Ge(Se_{1/2})_4$ tetrahedra and $Se_{3/2}Ge–GeSe_{3/2}$ ethane-like dimers. The concentration of homopolar bonds we measure is inconsistent with the random covalent network model (Liang *et al* 1974, Elliott 1990) in which the distribution of bond types is purely statistical and the ratio of the number of Ge–Ge (or Se–Se) bonds to the total number of bonds, $N_{\mathrm{Ge-Ge}}/N_{bond}$, is 25%. The present results are also inconsistent with the chemically ordered network model (White 1974, Elliott 1990) in which homopolar bonds are absent at the $GeSe_2$ composition.

The comparison of table 3 shows that, although there is a broad consensus between the results obtained from many techniques on the number of Ge involved in ES $Ge(Se_{1/2})_4$ tetrahedra, the number of Ge involved in dimers varies considerably. For example, our neutron diffraction work gives $N_{\mathrm{Ge}}(\mathrm{dimer})/N_{\mathrm{Ge}} = 25(5)\%$ whereas the Raman and Mössbauer spectroscopy studies of Boolchand and Bresser (2000) give $N_{\mathrm{Ge}}(\mathrm{dimer})/N_{\mathrm{Ge}} = 15(2)\%$. Part of this disagreement may arise from the use of different quench rates and nascent liquid temperatures to prepare the glassy $GeSe_2$ samples. For example, the glass transition temperature T_g (onset) measured under identical scanning conditions in differential scanning calorimetry experiments was 394(6) °C for our samples and 413(2) °C for the samples of Boolchand and Bresser (2000), which is indicative of a faster quench rate in the present work. Furthermore, our samples were quenched from ≈110 °C above the liquidus whereas those of Boolchand and Bresser (2000) were quenched from 50 °C above the liquidus and the network structure of liquid $GeSe_2$ is known to break down and become more 'fragile' with increasing temperature; there is a collapse of the intermediate-range ordering and concomitant increase in the short-range chemical disorder (Petri *et al* 1999a, Massobrio *et al* 2000b). Thus it is feasible that a relatively large number of homopolar bonding defects were frozen into the glassy samples used for the present neutron diffraction experiments to give a homopolar bond concentration in agreement with the law of mass action estimate (Feltz 1985). The degree of broken chemical order might be reduced by annealing the $GeSe_2$ samples used in our neutron diffraction experiment below the glass transition temperature (cf Nemanich *et al* (1978)).

The comparison of table 3 also shows that the measured ratio for the number of Ge involved in ES and CS tetrahedra, $N_{\mathrm{Ge}}(\mathrm{ES})/N_{\mathrm{Ge}}(\mathrm{CS})$, can vary considerably from the value of unity

[1] In a recent EXAFS experiment on amorphous thin films of $Ge_{0.32}Se_{0.68}$ prepared by *sputtering*, homopolar bonds with comparable bonding distances and coordination numbers to the present work were observed (Choi *et al* 2002).

found in HT-$GeSe_2$ (Dittmar and Schäfer 1976). The present experimental work on glassy $GeSe_2$ is in fair accord with $N_{Ge}(ES)/N_{Ge}(CS) = 1$ and the neutron diffraction work of Penfold and Salmon (1991) on the liquid phase of $GeSe_2$ is also consistent with $N_{Ge}(ES) \approx N_{Ge}(CS)$.

We also find evidence for a Ge–Se defect peak at 3.02(2) Å, a value that is too short for an intra-molecular distance in $Se_{3/2}Ge$–$GeSe_{3/2}$ ethane-like dimers, which suggests that some of the $Ge(Se_{1/2})_4$ tetrahedra are strongly distorted (Cobb *et al* 1996, Petri *et al* 2000). However, unlike the homopolar bonding features in the like-atom $g'_{\alpha\beta}(r)$, this defect peak is not readily discernible in $g'_{GeSe}(r)$ owing to the substantial effect of $M(r)$ on the first peak in the Ge–Se partial pair distribution function. Moreover, the peak gives a Ge–Se coordination number of 0.29(5) that is too large to be consistent with four-fold coordinated Ge, i.e. there is doubt regarding its magnitude. Planned experiments to measure the full set of partial structure factors for glassy $GeSe_2$ up to much higher k values will reduce the size of the $M(r)$ modification function and thereby shed more definitive light on this feature.

5.2. Comparison of the measured structures for glassy and liquid $GeSe_2$ with first-principles molecular dynamics simulations

It is interesting to compare the neutron diffraction results for glassy and liquid $GeSe_2$ with the results obtained from recent first principles molecular dynamics simulations. Unlike molecular dynamics simulations based on classical inter-atomic potentials (Vashishta *et al* 1989a, 1989b), several of the important features observed in the diffraction experiments are reproduced to a greater or lesser extent. For example, the classical molecular dynamics simulations did not find homopolar bonds, three-body terms had to be induced to increase the ratio of ES to CS tetrahedra closer to experimental estimates and an FSDP in the Bhatia and Thornton (1970) concentration–concentration partial structure factor $S^{BT}_{CC}(k)$ was not observed. Indeed, the absence of this feature was considered to be *generic* for AX_2 systems (Vashishta *et al* 1990, Iyetomi *et al* 1991). Nevertheless, the study of $GeSe_2$ by first-principles molecular dynamics simulation has proved challenging and two different approaches have been adopted (Drabold *et al* 2003, Massobrio *et al* 2003). In one approach it is found that the generalized gradient approximation in density functional theory, which enhances the ionic character of the bonding with respect to the local density approximation, is required to produce the best agreement with experiment (Massobrio *et al* 1998, 1999, 2000a, 2001). In the other approach it is found that a model computed with the Harris functional in the local density approximation can reproduce many of the features observed experimentally (Cobb *et al* 1996, Cobb and Drabold 1997, Zhang and Drabold 2000).

The full set of partial structure factors $S_{\alpha\beta}(k)$ and corresponding $g_{\alpha\beta}(r)$ for both the glassy (present work) and liquid (Penfold and Salmon 1991) phases of $GeSe_2$ are presented in figure 7. Since the diffraction results for the glassy phase of $GeSe_2$ show clear homopolar bonding features, the like-atom $g_{\alpha\beta}(r)$ obtained from a maximum entropy analysis of the liquid phase data are presented in which the existence of homopolar bonds was explored by reducing the low-r cut-off distances for $g_{GeGe}(r)$ and $g_{SeSe}(r)$ (see Penfold and Salmon1991 for details). The corresponding peak positions and coordination numbers are given in table 2. The experimental data for the glass are compared with the molecular dynamics simulation results of Zhang and Drabold (2000) while those for the liquid are compared with the molecular dynamics simulation results of both Cobb and Drabold (1997) and Massobrio *et al* (2001).

A striking feature in the comparison of the experimental $S_{GeGe}(k)$ for the glassy and liquid phases is the FSDP (figure 7(a)). The position and half width at half maximum of the FSDP for the glass are 1.00(1) and 0.37(1) $Å^{-1}$, respectively, which compare with 0.98(2) and 0.40(2) $Å^{-1}$ for the liquid, and the height of the FSDP for the glass is 12(3)% higher. This

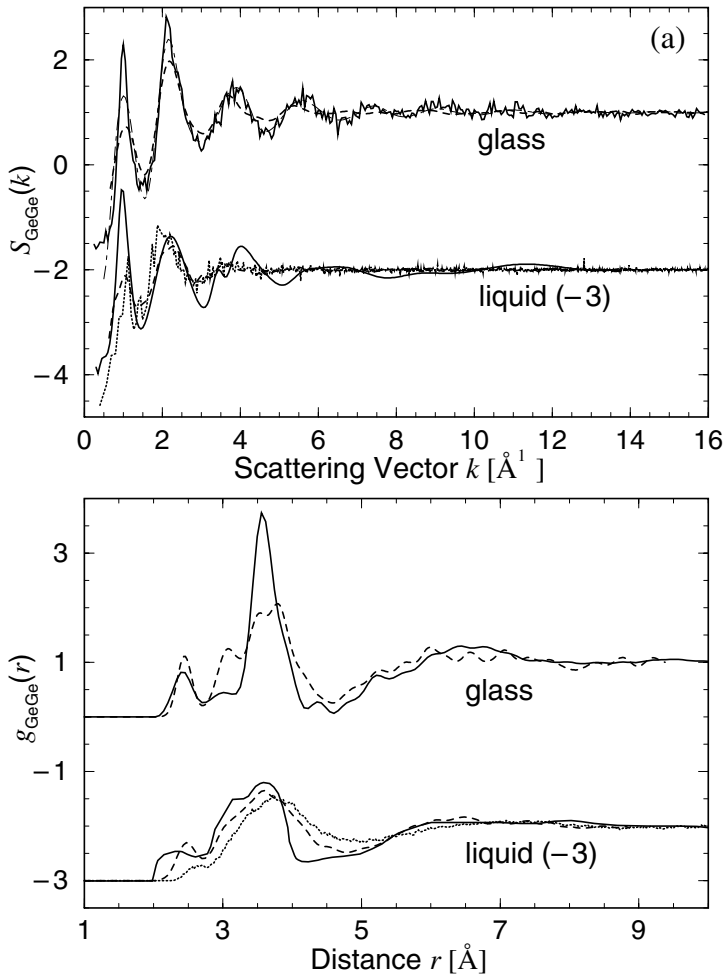

Figure 7. A comparison between the measured and simulated partial structure factors, $S_{\alpha\beta}(k)$, and partial pair distribution functions, $g_{\alpha\beta}(r)$, for the glassy and liquid phases of $GeSe_2$. The thick full curves represent the measured functions for either the glassy phase at 26(1) °C (present work) or the liquid phase at 784(3) °C (Penfold and Salmon 1991). For the glass, the thick broken curves are from the simulation of Zhang and Drabold (2000). For the liquid, the thick broken curves are from the simulation of Cobb and Drabold (1997) while the dotted curves are from the simulation of Massobrio *et al* (2001). For the liquid phase in (a), a spline fit to the experimental $S_{GeGe}(k)$ is shown for clarity of presentation. For the glassy phase in (a), the chain curve for $S_{GeGe}(k)$ is the back Fourier transform of the measured $g_{GeGe}(r)$ shown in the lower panel after it has been truncated at 8.2 Å (see the text).

observation is consistent with previous neutron diffraction work at the *total* structure factor level (Susman *et al* 1988, 1990) where it was found that the height of the FSDP in the liquid at 1084 K is only 10% less than in the glass at 10 K and that there is little change in its position and width. By comparison, on progressing from the glass to the liquid, a decrease of the FSDP position might be expected from the thermal expansion of the system and a significant reduction of the FSDP height anticipated from the increased thermal disorder (see e.g. Salmon 1994). A more ordered distribution of the Ge-centred $Ge(Se_{1/2})_4$ units can, however, be explained in terms of a relaxation of the network (due to thermal expansion) which has a

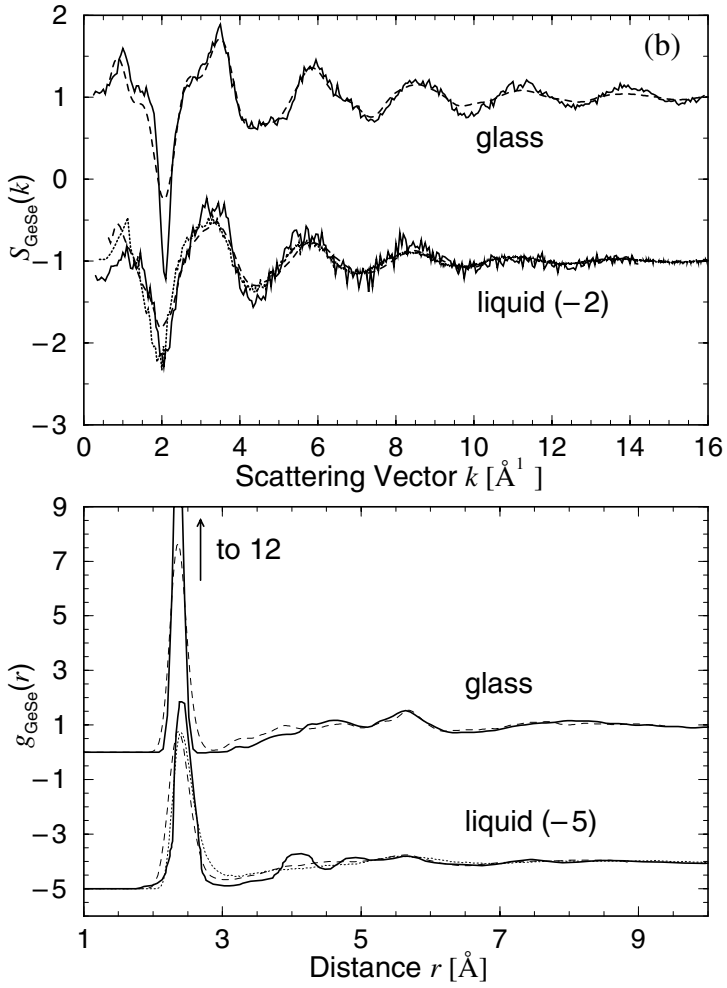

Figure 7. (Continued.)

more pronounced ordering influence than the disorder caused by increased thermal vibrations. Vashishta *et al* (1989a, 1989b) found this effect in their molecular dynamics simulations of $GeSe_2$ and refer to it as a reduction with decreasing density of the 'frustration' associated with the packing of the $Ge(Se_{1/2})_4$ units.

The agreement between the measured and molecular dynamics $S_{GeGe}(k)$ for both the liquid and glassy phases is unsatisfactory. In the case of the liquid, the measured FSDP is poorly reproduced and the other simulated k-space features are too damped. For the glass, the simulated FSDP is again too small and the other features are too liquid-like, reflecting the short quench times used in molecular dynamics simulations (see e.g. Drabold *et al* 2003). The discrepancy between experiment and simulation in the FSDP region *cannot* be solely attributed to finite size effects in the latter. This can be demonstrated by Fourier transforming the experimentally deduced $g_{GeGe}(r)$ of figure 6(a) after truncating it at a node near 8 Å, a distance much *shorter* than the value of $\approx 2L/3 = 12.5$ Å (Cobb *et al* 1996, Zhang and Drabold 2000) for which reliable statistics can be gathered between independent atoms in a cubic super cell of side length L (Galli and Parrinello 1991). By contrast to simulation, the

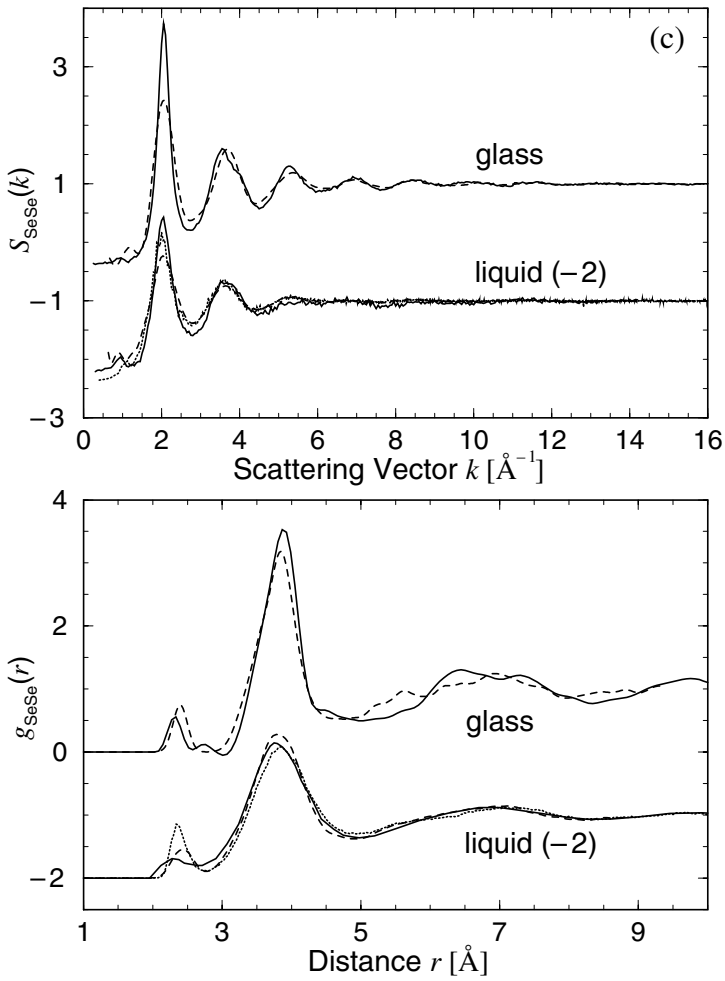

Figure 7. (Continued.)

modified Ge–Ge partial structure factor thus deduced gives a much better representation of the first two peaks in the measured $S_{GeGe}(k)$—see figure 7(a).

The peaks in the measured $g_{GeGe}(r)$ for the glass are sharper than for the liquid but yield comparable coordination numbers (table 2). For the liquid, the simulated $g_{GeGe}(r)$ of Cobb and Drabold (1997) is shifted to smaller r, when compared with the simulated $g_{GeGe}(r)$ of Massobrio *et al* (2001), in better agreement with experiment. The first main peak in both simulations does, however, give a distribution of Ge–Ge neighbours that is too broad. For the glass, the simulated $g_{GeGe}(r)$ is roughly comparable with experiment but the features are, overall, too liquid-like. A distribution of nearest-neighbour distances between Ge-centred structural motifs that is too smeared would help explain the inability of the molecular dynamics simulations to reproduce the measured FSDP in $S_{GeGe}(k)$ by leading to a structure that is too disordered at intermediate ranged distances.

The features in the measured $S_{GeSe}(k)$ for the glass are more pronounced than for the liquid and give a first peak in $g_{GeSe}(r)$ having a higher intensity, larger coordination number and a position that is shifted to smaller r (table 2). By comparison with the Ge–Ge correlation functions, the molecular dynamics simulations give $S_{GeSe}(k)$ and $g_{GeSe}(r)$ for the liquid phase

that are in better agreement with experiment. Nevertheless, the molecular dynamics results for the Ge–Se correlations in the glassy phase are again too liquid-like.

The measured $S_{SeSe}(k)$ for the glassy and liquid phases both show a small FSDP at 0.95(2) and 0.94(2) $Å^{-1}$, respectively, and higher k features that are more strongly damped for the liquid. The corresponding r-space functions for both phases each show homopolar bonds and, while the features in $g_{SeSe}(r)$ are broader for the liquid, comparable nearest-neighbour coordination numbers are obtained (table 2). For the liquid, both sets of molecular dynamics results are in fair agreement with experiment in real and reciprocal space although the simulation of Massobrio *et al* (2001) gives a homopolar bonding feature in $g_{SeSe}(r)$ that is too sharp. Again, the simulated results for the glassy phase are, on the whole, too liquid-like.

It is notable that, for liquid GeSe, the largest discrepancy between the measured $S_{\alpha\beta}(k)$ (Petri *et al* 1999c) and those calculated using first-principles molecular dynamics methods (van Roon *et al* 2000, Raty *et al* 2001) again occurs with respect to the Ge–Ge correlations. In real space, the simulated $g_{GeGe}(r)$ gives a distribution of Ge–Ge nearest neighbours that is too broad and featureless and the measured homopolar bonding feature in $g_{SeSe}(r)$ was not reproduced. Good agreement between the experimental and simulated $g_{GeSe}(r)$ was, however, found.

5.3. Experimental and simulated Bhatia–Thornton partial structure factors for glassy and liquid $GeSe_2$

The measured Bhatia and Thornton (1970) partial structure factors for glassy and liquid $GeSe_2$ are, in accordance with the Faber–Ziman $S_{\alpha\beta}(k)$, sharper for the glassy phase (figure 8). The FSDP in $S_{NN}^{BT}(k)$, which dominates the function ${}_N^N F(k)$ measured in conventional neutron diffraction experiments, is positioned at 1.00(2) $Å^{-1}$ for the glass and at 0.98(2) $Å^{-1}$ for the liquid and its height in the liquid phase is reduced by about 15%. This observation, together with the disappearance of the high-k shoulder on the fourth peak upon melting, is in broad agreement with the previous neutron diffraction experiments of Susman *et al* (1988, 1990).

It is of particular interest to compare $S_{CC}^{BT}(k)$ for the glassy and liquid phases since Penfold and Salmon (1991) observed an FSDP at about 1 $Å^{-1}$ for the melt, which implies that there are concentration fluctuations on the scale of the intermediate-range order. A subsequent analysis by Salmon (1992) of the full set of measured partial structure factors for liquid AX_2 systems within the Bhatia–Thornton formalism showed that an FSDP in $S_{CC}^{BT}(k)$ also occurs for other systems such as the network glass forming liquid $ZnCl_2$. This feature does *not*, however, appear in integral equation calculations (Iyetomi *et al* 1989, 1991) or classical molecular dynamics simulations (Vashishta *et al* 1990) of amorphous $GeSe_2$ and it has proved difficult to reproduce this feature using the first-principles molecular dynamics approach of Massobrio *et al* (1998, 2000a, 2003).

As shown in figure 8, the new experimental results for the glassy phase of $GeSe_2$ also show an FSDP in $S_{CC}^{BT}(k)$. Its position, full width at half maximum and height are 1.00(2) $Å^{-1}$, 0.37(5) $Å^{-1}$ and 0.13(1), respectively, which compare with 0.95(2) $Å^{-1}$, 0.36(5) $Å^{-1}$ and 0.15(2) for the liquid. In figure 9, $S_{CC}^{BT}(k)$ for the glass is compared with the first-principles molecular dynamics simulation results of Zhang and Drabold (2000) while $S_{CC}^{BT}(k)$ for the liquid is compared with the molecular dynamics simulation results of both Cobb and Drabold (1997) and Massobrio *et al* (2001). Although the simulation results for the glass are too liquid-like, an FSDP in better agreement with experiment is observed. Since it can be shown that (Bhatia and Thornton 1970)

$$S_{CC}^{BT}(k) = c_{Ge}c_{Se}\{1 + c_{Ge}c_{Se}[S_{GeGe}(k) + S_{SeSe}(k) - 2S_{GeSe}(k)]\}, \tag{14}$$

the origin of the discrepancy between experiment and simulation can be traced in large part

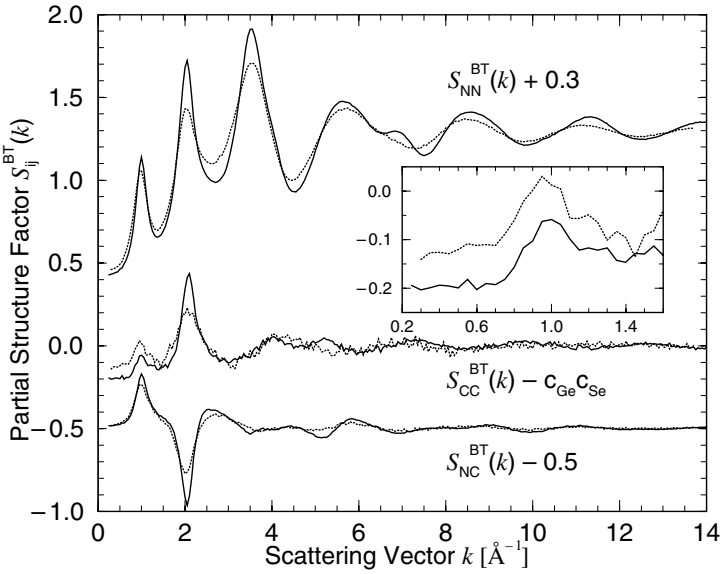

Figure 8. Comparison of the measured Bhatia–Thornton partial structure factors, $S_{ij}^{BT}(k)$, for the glassy phase of $GeSe_2$ at 26(1) °C (full curves—present work) and the liquid phase of $GeSe_2$ at 784(3) °C (dotted curves—Penfold and Salmon (1991)). The inset shows the region of the FSDP in $S_{CC}^{BT}(k)$ on an enlarged scale.

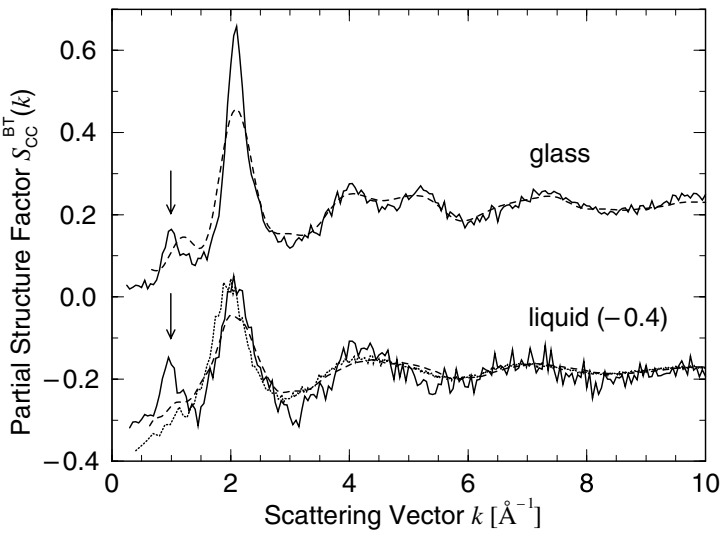

Figure 9. A comparison between the measured and simulated Bhatia–Thornton concentration–concentration partial structure factor, $S_{CC}^{BT}(k)$, for the glassy and liquid phases of $GeSe_2$. The thick full curves represent the measured function for either the glassy phase (present work) or liquid phase (Penfold and Salmon 1991). For the glass, the broken curve is from the simulation of Zhang and Drabold (2000). For the liquid, the broken curve is from the simulation of Cobb and Drabold (1997) while the dotted curve is from the simulation of Massobrio *et al* (2001). The vertical arrows point to the FSDPs in the experimental data.

to the inadequacy of the latter to reproduce the FSDP in $S_{\mathrm{GeGe}}(k)$. The appearance of the FSDP in $S_{CC}^{BT}(k)$ presumably relates to the directional bonding with a high degree of covalent

character in $GeSe_2$ that yields both ES and CS Ge-centred tetrahedra which arrange to form a relatively open network and a non-uniform concentration of Ge and Se atoms on the scale of the intermediate-range order (Salmon 1992).

6. Conclusions

The full set of partial structure factors has been measured for the network glass forming system $GeSe_2$. The results show that the basic building block is the $Ge(Se_{1/2})_4$ tetrahedron in which 34(5)% of the Ge reside in ES configurations. The intrinsic chemical order of the glass is, however, broken with a maximum of 25(5)% Ge and 20(5)% Se being involved in homopolar bonds, consistent with the existence of these features in the liquid phase of $GeSe_2$. An FSDP in the Bhatia–Thornton concentration–concentration partial structure factor is also observed for the glassy phase and has a dominant contribution from the Ge–Ge correlations.

A comparison is made between the experimental data for the glassy and liquid phases of $GeSe_2$ and the results obtained from recent first-principles molecular dynamics simulations. It is found that the largest disagreement occurs with respect to the Ge–Ge correlations as for the case of liquid GeSe. Furthermore, the failure of the simulations to reproduce the large FSDP in $S_{GeGe}(k)$ does not arise from the finite size of the simulation box. Moreover, the simulated results for the glassy phase are too liquid-like, reflecting the use of a quench time greatly in excess of that achieved experimentally. It is therefore a moot point as to the extent to which the simulated dynamics will be representative of glassy $GeSe_2$.

Acknowledgments

It is a pleasure to thank Dr Henry Fischer for his help in the earlier stages of this work and Professors Dave Drabold and Carlo Massobrio for providing the results from their molecular dynamics simulations.

References

Angell C A 1988 *J. Phys. Chem. Solids* **49** 863
Azoulay R, Thibierge H and Brenac A 1975 *J. Non-Cryst. Solids* **18** 33
Benmore C J 1993 *PhD Thesis* University of East Anglia, UK
Benmore C J and Salmon P S 1994 *Phys. Rev. Lett.* **73** 264
Bertagnolli H, Chieux P and Zeidler M D 1976 *Mol. Phys.* **32** 759
Bhatia A B and Thornton D E 1970 *Phys. Rev.* B **2** 3004
Biggin S and Enderby J E 1981 *J. Phys. C: Solid State Phys.* **14** 3129
Boolchand P (ed) 2000 *Insulating and Semiconducting Glasses* (Singapore: World Scientific)
Boolchand P, Grothaus J, Bresser W J and Suranyi P 1982 *Phys. Rev.* B **25** 2975
Boolchand P, Grothaus J and Phillips J C 1983 *Solid State Commun.* **45** 183
Boolchand P and Phillips J C 1992 *Phys. Rev. Lett.* **68** 252
Boolchand P and Bresser W J 2000 *Phil. Mag.* B **80** 1757
Bresser W J, Boolchand P, Suranyi P and de Neufville J P 1981 *Phys. Rev. Lett.* **46** 1689
Bresser W J, Boolchand P, Suranyi P and Hernandez J G 1986 *Hyperfine Interact.* **27** 389
Bridenbaugh P M, Espinosa G P, Griffiths J E, Phillips J C and Remeika J P 1979 *Phys. Rev.* B **20** 4140
Choi J, Gurman S J and Davis E A 2002 *J. Non-Cryst. Solids* **297** 156
Cobb M and Drabold D A 1997 *Phys. Rev.* B **56** 3054
Cobb M, Drabold D A and Cappelletti R L 1996 *Phys. Rev.* B **54** 12162
Crichton W A, Mezouar M, Grande T, Stølen S and Grzechnik A 2001 *Nature* **414** 622
Dittmar G and Schäfer H 1976 *Acta Crystallogr.* B **32** 2726
Drabold D A, Li Jun and De Nyago Tafen 2003 *J. Phys.: Condens. Matter* **15** S1529
Durandurdu M and Drabold D A 2002 *Phys. Rev.* B **65** 104208
Edwards F G, Enderby J E, Howe R A and Page D I 1975 *J. Phys. C: Solid State Phys.* **8** 3483
Elliott S R 1990 *Physics of Amorphous Materials* 2nd edn (New York: Longman)

Elliott S R 1991 *Nature* **354** 445
Faber T E and Ziman J M 1965 *Phil. Mag.* **11** 153
Feltz A 1985 *Physics of Disordered Materials* ed D Adler, H Fritzsche and S R Ovshinsky (New York: Plenum) p 203
Feltz A 1993 *Amorphous Inorganic Materials and Glasses* (Weinheim: VCH)
Feltz A, Pohle M, Steil H and Herms G 1985 *J. Non-Cryst. Solids* **69** 271
Fischer-Colbrie A and Fuoss P H 1990 *J. Non-Cryst. Solids* **126** 1
Fuoss P H, Eisenberger P, Warburton W K and Bienenstock A 1981 *Phys. Rev. Lett.* **46** 1537
Galli G and Parrinello M 1991 *J. Chem. Phys.* **95** 7504
Iyetomi H, Vashishta P and Kalia R K 1989 *J. Phys.: Condens. Matter* **1** 2103
Iyetomi H, Vashishta P and Kalia R K 1991 *Phys. Rev.* B **43** 1726
Jackson K, Briley A, Grossman S, Porezag D V and Pederson M R 1999 *Phys. Rev.* B **60** R14985
Jackson K, Srinivas S, Kortus J and Pederson M 2002 *Phys. Rev.* B **65** 214201
Jal J F, Mathieu C, Chieux P and Dupuy J 1990 *Phil. Mag.* B **62** 351
Liang K S, Bienenstock A and Bates C W 1974 *Phys. Rev.* B **10** 1528
Liu J and Salmon P S 1997 *Europhys. Lett.* **39** 521
Mamedov S B, Aksenov N D, Makarov L L and Batrakov Yu F 1996 *J. Non-Cryst. Solids* **195** 272
Massobrio C, Celino M and Pasquarello A 2003 *J. Phys.: Condens. Matter* **15** S1537
Massobrio C, Pasquarello A and Car R 1998 *Phys. Rev. Lett.* **80** 2342
Massobrio C, Pasquarello A and Car R 1999 *J. Am. Chem. Soc.* **121** 2943
Massobrio C, Pasquarello A and Car R 2000a *Comput. Mater. Sci.* **17** 115
Massobrio C, Pasquarello A and Car R 2001 *Phys. Rev.* B **64** 144205
Massobrio C, van Roon F H M, Pasquarello A and De Leeuw S W 2000b *J. Phys.: Condens. Matter* **12** L697
Moss S C and Price D L 1985 *Physics of Disordered Materials* ed D Adler, H Fritzsche and S R Ovshinsky (New York: Plenum) p 77
Murase K 2000 *Insulating and Semiconducting Glasses* ed P Boolchand (Singapore: World Scientific) p 415
Nemanich R J, Connell G A N, Hayes T M and Street R A 1978 *Phys. Rev.* B **18** 6900
Nemanich R J, Galeener F L, Mikkelsen J C Jr, Connell G A N, Etherington G, Wright A C and Sinclair R N 1983 *Physica* B **117/118** 959
Penfold I T and Salmon P S 1990 *J. Phys.: Condens. Matter* **2** SA233
Penfold I T and Salmon P S 1991 *Phys. Rev. Lett.* **67** 97
Penfold I T and Salmon P S 1992 *Phys. Rev. Lett.* **68** 253
Peters M J and McNeil L E 1992 *J. Non-Cryst. Solids* **139** 231
Petri I and Salmon P S 2002 *Phys. Chem. Glasses* **43C** 185
Petri I, Salmon P S and Howells W S 1999a *J. Phys.: Condens. Matter* **11** 10219
Petri I, Salmon P S and Fischer H E 1999b *J. Non-Cryst. Solids* **250–252** 405
Petri I, Salmon P S and Fischer H E 1999c *J. Phys.: Condens. Matter* **11** 7051
Petri I, Salmon P S and Fischer H E 2000 *Phys. Rev. Lett.* **84** 2413
Raty J Y, Godlevsky V V, Gaspard J P, Bichara C, Bionducci M, Bellissent R, Céolin R, Chelikowsky J R and Ghosez Ph 2001 *Phys. Rev.* B **64** 235209
Salmon P S 1988 *J. Phys. F: Met. Phys.* **18** 2345
Salmon P S 1992 *Proc. R. Soc.* A **437** 591
Salmon P S 1994 *Proc. R. Soc.* A **445** 351
Salmon P S and Benmore C J 1992 *Recent Developments in the Physics of Fluids* ed W S Howells and A K Soper (Bristol: Adam Hilger) p F225
Salmon P S and Liu J 1994 *J. Phys.: Condens. Matter* **6** 1449
Salmon P S and Xin S 2002 *Phys. Rev.* B **65** 064202
Salmon P S, Xin S and Fischer H E 1998 *Phys. Rev.* B **58** 6115
Sears V F 1992 *Neutron News* **3** 26
Sinclair R N, Wright A C, Clare A G and Hannon A C 2002 *Phys. Chem. Glasses* **43C** 191
Stølen S, Grande T and Johnsen H-B 2002 *Phys. Chem. Chem. Phys.* **4** 3396
Sugai S 1987 *Phys. Rev.* B **35** 1345
Susman S, Price D L, Volin K J, Dejus R J and Montague D G 1988 *J. Non-Cryst. Solids* **106** 26
Susman S, Volin K J, Montague D G and Price D L 1990 *J. Non-Cryst. Solids* **125** 168
Tronc P, Bensoussan M, Brenac A and Sebenne C 1973 *Phys. Rev.* B **8** 5947
van Roon F H M, Massobrio C, de Wolff E and De Leeuw S W 2000 *J. Chem. Phys.* **113** 5425
Vashishta P, Kalia R K, Antonio G A and Ebbsjö I 1989a *Phys. Rev. Lett.* **62** 1651
Vashishta P, Kalia R K and Ebbsjö I 1989b *Phys. Rev.* B **39** 6034
Vashishta P, Kalia R K, Rino J P and Ebbsjö I 1990 *Phys. Rev.* B **41** 12197
White R M 1974 *J. Non-Cryst. Solids* **16** 387
Zachariasen W H 1932 *J. Am. Chem. Soc.* **54** 3841
Zhang X and Drabold D A 2000 *Phys. Rev.* B **62** 15695
Zhou W, Paesler M and Sayers D E 1991 *Phys. Rev.* B **43** 2315